

MindScan: Dual Deep Learning system of Brain Tumors Detection and Classification from MRI Scans

BAZGOUR YASSINE¹, ABOUHANE ZAHRA¹, AND QAFFOU ISSAM¹

¹ Semlalia Faculty, Department of Computer Science, Cadi Ayyad University, Marrakesh, Morocco

This project presents MindScan, a web-based hierarchical deep learning system for automated brain tumor detection and classification from MRI images, using MobileNetV2 as the primary model. MRI scans were preprocessed with grayscale conversion, black-border cropping, CLAHE contrast enhancement, bilateral denoising, and intensity normalization to improve feature consistency and generalization. The pipeline employs a dual-stage architecture: a binary classifier detects tumor versus non-tumor cases, followed by a multi-class classifier distinguishing glioma, meningioma, and pituitary tumors. MobileNetV2 trained on preprocessed data achieved 99% validation accuracy for binary classification and 91.3% for multi-class classification. The web interface allows users to upload MRI images and receive real-time predictions, demonstrating reliable performance across diverse tumor types. These results highlight the effectiveness of combining preprocessing, a hierarchical architecture, and a lightweight CNN for accurate, efficient, and accessible brain tumor detection suitable for clinical and real-time applications.

21 B. Aim

22 The primary aim of this project is to develop an intelligent diagnostic system for brain tumor detection and classification using
 23 MRI images. The approach focuses on analyzing high-resolution
 24 brain MRI scans to automatically identify and differentiate be-
 25 tween normal and abnormal cases. The system employs a dual-
 26 structured deep learning architecture, integrating both binary
 27 classification (normal vs. tumor) and multi-class classification
 28 (Glioma, Meningioma, Pituitary) models. This structure enables
 29 the system to first determine the presence of a tumor, and then
 30 accurately classify its specific type, enhancing diagnostic preci-
 31 sion and clinical applicability. Furthermore, the project aims to
 32 integrate this model into a web-based platform called MindScan,
 33 providing an accessible interface for radiologists and healthcare
 34 professionals to facilitate early brain tumor detection, streamline
 35 diagnosis, and support remote medical assessment.
 36

37 C. Related Work

38 Recent research on MRI-based brain tumor analysis focuses
 39 on improving diagnostic accuracy, segmentation quality, and
 40 model reliability. Three representative works illustrate the main
 41 directions in the field.

42 **Explainable ConvMixer-Based Classification Models** Selva
 43 Birunda et al. [1] in 2025 proposed EM-ConvMixer+Net, an
 44 explainable framework combining ConvMixer blocks with atten-
 45 tion mechanisms to improve classification and interpretability.
 46 The model achieves high accuracy and provides visual expla-
 47 nations through Grad-CAM, but its multi-module architecture
 48 increases implementation complexity and computational cost.

49 **YOLO-Based Real-Time Tumor Detection** Nuthi Raju et al.
 50 [2] in 2025 introduced YOLO-Beta11, a lightweight model de-
 51 signed for real-time tumor detection. It integrates attention-
 52 enhanced modules and optimized loss functions, achieving
 53 strong precision and recall while keeping inference efficient.
 54 However, as a single-stage detector, it outputs bounding boxes
 55 rather than detailed tumor masks, limiting its use for tasks re-
 56 quiring pixel-level segmentation.

57 **Hybrid VGG16-InceptionV3 Feature Fusion Models** Jamaa
 58 et al. [3] in 2025 as well, developed a hybrid model that merges
 59 VGG16 and InceptionV3 features for multi-class tumor classifi-
 60 cation. This fusion improves generalization and boosts accuracy
 61 across tumor types. The drawback is the increased model size,
 62 which makes deployment slower and less suitable for resource-
 63 constrained clinical environments.

2

3

4 1. INTRODUCTION

5 A. Problem

6 Brain tumors such as gliomas, meningiomas, and pituitary tu-
 7 mors remain difficult to diagnose early, and they often lead
 8 to severe health outcomes when detected late. Even experi-
 9 enced radiologists can misinterpret MRI scans, especially when
 10 small or subtle abnormalities are present. This challenge is more
 11 pronounced in regions with limited access to specialized radio-
 12 logical expertise, where delays and diagnostic errors are more
 13 common.

14 Traditional diagnosis depends heavily on human interpreta-
 15 tion, which is time-consuming, costly, and prone to subjectivity.
 16 As a result, many patients do not receive timely and accurate
 17 assessments. There is a clear need for intelligent, automated
 18 systems capable of analyzing MRI scans with high precision,
 19 detecting minute patterns that may escape the human eye, and
 20 supporting clinicians in making faster, more reliable decisions.

64 2. METHODOLOGY

65 A. Data

66 A.1. Data Overview

67 The experiments use the Brain Tumor MRI Dataset by Masoud
 68 Nickparvar from Kaggle [4], which includes MRI images la-
 69 beled as glioma, meningioma, pituitary tumor, and no tumor.
 70 Although the dataset provider indicates uniform dimensions,
 71 verification confirmed that all images are consistently sized at
 72 224×224. The original Training and Testing folders were merged
 73 into a single pool, and the final train-validation-test split was
 74 performed programmatically within the code. Since the images
 75 already share the same resolution, only normalization was ap-
 76 plied before feeding them into the models. This setup ensures a
 77 clean, unified dataset suitable for both detection and classifica-
 78 tion tasks.

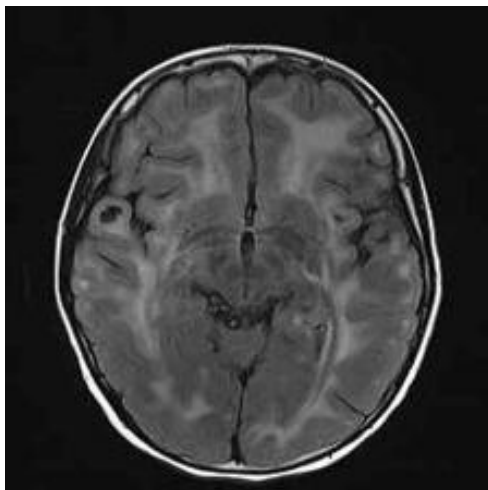


Fig. 1. Normal brain MRI scan with symmetrical structure and no visible abnormal growths or irregularities.

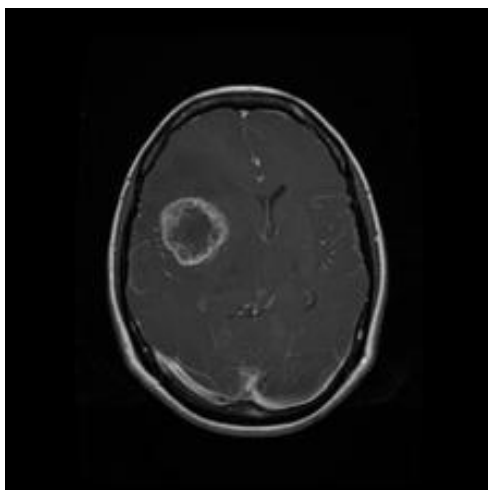


Fig. 2. MRI scan showing an abnormal brain region characterized by irregular mass and tissue deformation, indicative of a brain tumor.

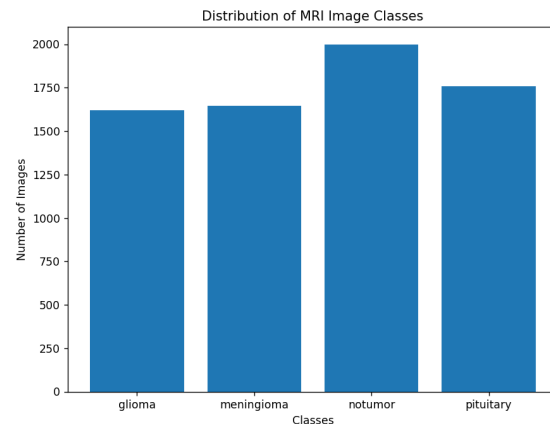


Fig. 3. This graph shows the distribution of the 4 classes, normal and 3 abnormal classes through the dataset

79 A.2. Data Preprocessing

80 The original MRI dataset presents substantial variability in res-
 81 olution, field-of-view, contrast distribution, and noise levels
 82 across subjects and acquisition devices. To obtain standard-
 83 ized, noise-reduced, and contrast-enhanced inputs suitable for
 84 CNN-based tumor classification, we designed a deterministic
 85 preprocessing pipeline applied to every image in dataset. All
 86 steps were implemented in Python using OpenCV.

87 The complete pipeline consists of the following stages:

- 88 1. **Grayscale Loading** All MRI slices were loaded in grayscale
 89 using OpenCV. This ensures a uniform single-channel input
 90 representation across all samples.

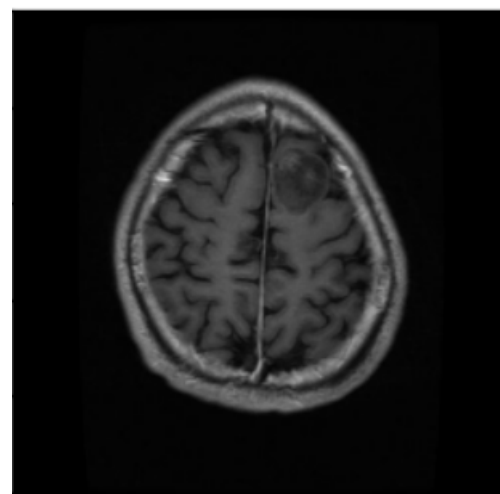


Fig. 4. Original input MRI

- 91 2. **Automatic Black-Border Cropping** Many MRI images con-
 92 tain large black margins surrounding the head. To remove
 93 these regions, we applied a morphological bounding-box
 94 cropping. This step isolates the brain region, reduces irrele-
 95 vant background, and improves consistency across scans.

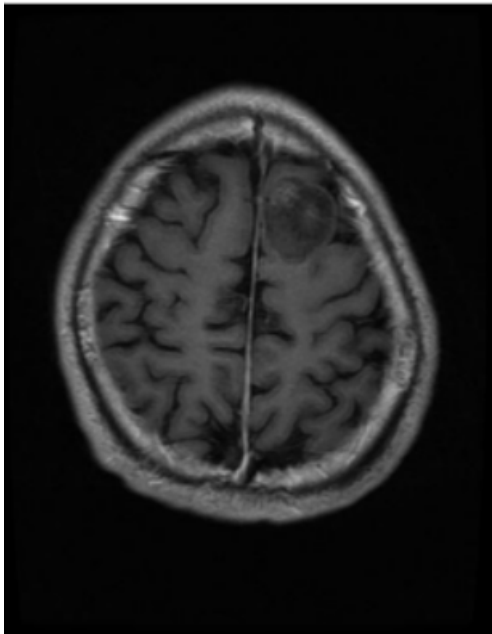


Fig. 5. Output after black-border cropping

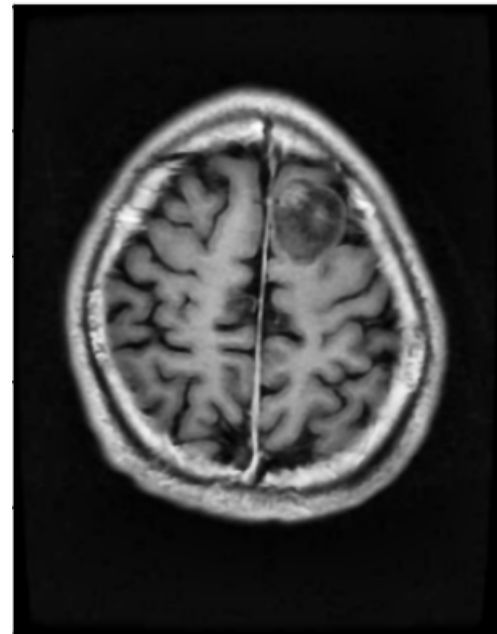


Fig. 7. Output after bilateral filtering

96 3. **Local Contrast Enhancement (CLAHE)** To handle contrast 107
97 heterogeneity between MRI scanners, we applied Contrast 108
98 Limited Adaptive Histogram Equalization (CLAHE) with 109
99 the following parameters: CLAHE locally boosts visibility 110
100 of structures by enhancing edges and intensities without 111
101 amplifying noise excessively. 112

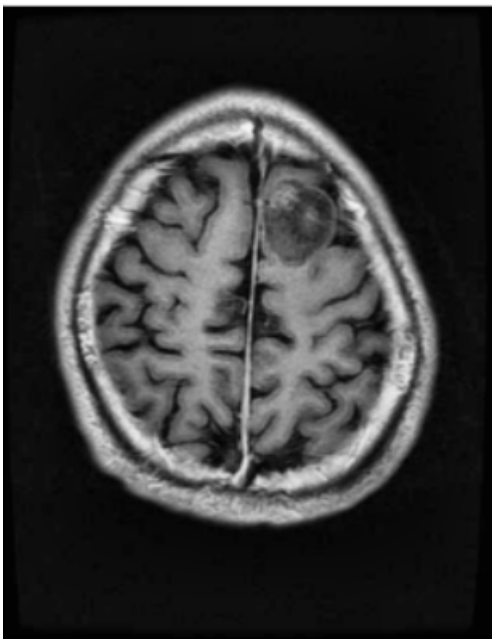


Fig. 6. Output after CLAHE

102 4. **Edge-Preserving Denoising (Bilateral Filter)** Following 103
104 contrast enhancement, residual noise is smoothed using a 105
106 bilateral filter: This filter reduces noise while preserving 107
108 anatomical edges, unlike Gaussian blur which smooths 109
110 edges away. 111

5. **Intensity Normalization** Before saving the preprocessed 112
113 images, each image was normalized to the range [0, 1]. This 114
115 normalization ensures stable numerical behavior during 116
117 model training and keeps pixel intensities consistent across 118
119 the dataset. These preprocessed images were then saved 120
121 back as uint8 images (scaled back to 0–255 only for storage), 122
123 while the internal normalized representation is used for 124
125 model input. 126

6. **Secondary Normalization (Step 2: Conversion to .npy for 127
128 Training)** A second normalization stage was executed to 129
130 prepare the final model input. 131

A.3. Dataset Configuration for Classification Tasks

Tumor vs No-tumor Binary Classification For implementing 132
133 binary classification we splitted the dataset to contains all 2000 134
135 sample of no tumor class and a chunk of each tumor class, and 136
137 to make the dataset balanced between tumor and no tumor we 138
139 managed to take 667 sample of each three tumor classes which 140
141 resulted of 2001 sample. 142

Three-Class Tumor-Only Classification To classify tumor 143
144 type, samples from the notumor category are excluded. The 145
146 model learns to discriminate between: 147

- 148 • glioma
- 149 • meningioma
- 150 • pituitary tumor

151 This configuration focuses strictly on tumors and corresponds to 152
153 clinical tasks requiring tumor-type identification after a positive 154
155 detection. 156

157 **Train, Validation, and Test Split** The binary dataset is then 158
159 split into training, validation, and test sets using a reproducible 160
161 random seed. Stratified sampling ensures that both classes 162
163 maintain the same proportion in all splits. 164

165 This workflow prevents overfitting, stabilizes learning, and 166
167 provides a consistent framework for both binary and three-class 168
169 models. 170

141 classification tasks.

143 B. Models

144 B.1. Pipeline

145 The architecture follows a two-stage approach. First, a binary
 146 classifier determines whether an MRI scan is abnormal or normal.
 147 This step filters out healthy cases, **reducing unnecessary**
 148 **computation for normal images and improving overall detec-**
 149 **tion efficiency.** If the scan is classified as abnormal, it is passed
 150 to a multi-class classifier that distinguishes between the specific
 151 tumor types—glioma, meningioma, or pituitary tumor. This
 152 hierarchical design simplifies the classification task, allows the
 153 models to focus on relevant features at each stage, and improves
 154 both accuracy and interpretability. [5]

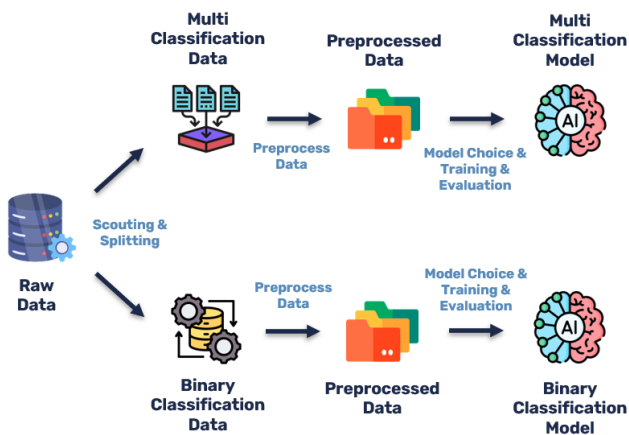


Fig. 8. Pipeline of models

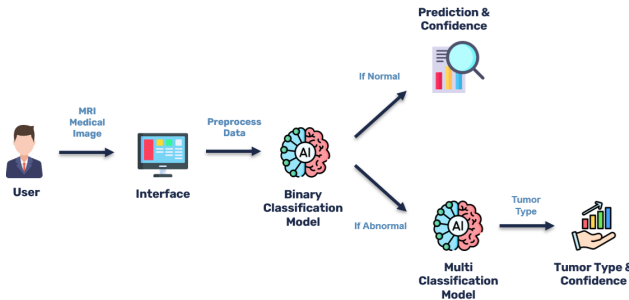


Fig. 9. User scenario

155 B.2. MobileNetV2

156 MobileNetV2 is a lightweight convolutional neural network
 157 designed for efficient performance on mobile and embedded
 158 devices. Introduced by Sandler et al. [6] in 2018, it uses inverted
 159 residual blocks with linear bottlenecks, preserving representa-
 160 tional power while reducing computation. MobileNetV2 has
 161 around 3.4 million parameters and a model size of approxi-
 162 mately 14 MB, making it highly compact compared to larger
 163 architectures like EfficientNetV2B0. It provides a strong balance
 164 of accuracy and speed, supporting real-time inference with low
 165 memory and computational requirements. Its main limitation is
 166 that it may not achieve the highest accuracy on very challenging
 167 datasets compared to larger models.

168 B.3. ResNet18

169 ResNet18 is a convolutional neural network introduced by He
 170 et al. [7] in 2016 that employs residual learning to facilitate the
 171 training of deeper networks. It consists of 18 layers with skip
 172 connections that allow gradients to flow more effectively during
 173 backpropagation, addressing the vanishing gradient problem
 174 common in deep architectures. ResNet18 has approximately 11.7
 175 million parameters, making it larger than MobileNetV2 but still
 176 relatively lightweight compared to deeper ResNet variants. It
 177 offers a strong trade-off between accuracy and computational
 178 efficiency, making it suitable for tasks requiring reliable feature
 179 extraction with moderate resources. Its main limitation is that
 180 it may be slower than extremely compact models on mobile or
 181 embedded devices.

182 B.4. EfficientNetV2B0

183 EfficientNetV2B0 is a state-of-the-art convolutional neural net-
 184 work that employs compound scaling of depth, width, and reso-
 185 lution to optimize accuracy and efficiency. It is designed to
 186 achieve high performance with fewer parameters and reduced
 187 computational cost compared to traditional large models. The
 188 architecture incorporates advanced features such as fused MB-
 189 Conv blocks and progressive learning rate scaling, making it
 190 well-suited for a variety of image classification tasks while main-
 191 taining a balance between model size, speed, and representa-
 192 tional power. [8]

193 C. Web Interface

194 The MindScan web interface provides a user-friendly platform
 195 for AI-based brain tumor detection. The frontend, built with
 196 HTML, CSS, and JavaScript, allows users to upload MRI images
 197 and receive predictions instantly. The backend, implemented in
 198 Python, processes the images and generates model outputs in
 199 real time through a lightweight API. [9], enabling fast, reliable,
 200 and accessible brain tumor analysis directly from the browser.

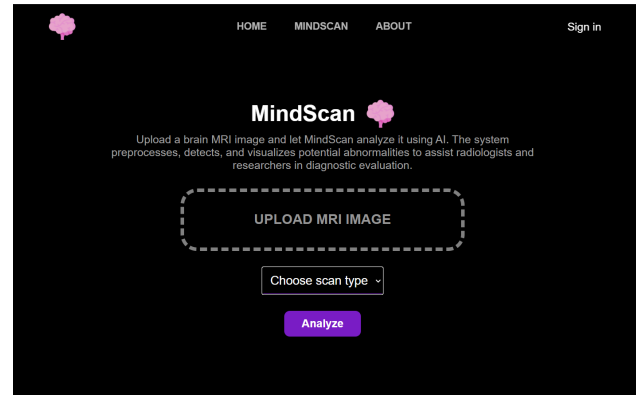


Fig. 10. MindScan interface.

201 3. RESULTS

202 A. Binary Classification with MobileNetV2

203 A.1. Applied on data not preprocessed

204 We trained MobileNetV2 as a binary classifier to distinguish
 205 between normal and abnormal MRI scans. The model achieved
 206 rapid convergence, reaching a training accuracy of 99.8% and a
 207 validation accuracy of 98.1% after 10 epochs. F1-score, precision,
 208 and recall metrics followed similar trends, with the final valida-
 209 tion F1-score reaching 0.981, demonstrating that MobileNetV2

210 can reliably detect abnormal scans. The training process was
 211 stable, with steadily decreasing loss, highlighting the efficiency
 212 and suitability of MobileNetV2 for real-time binary classification
 213 tasks.

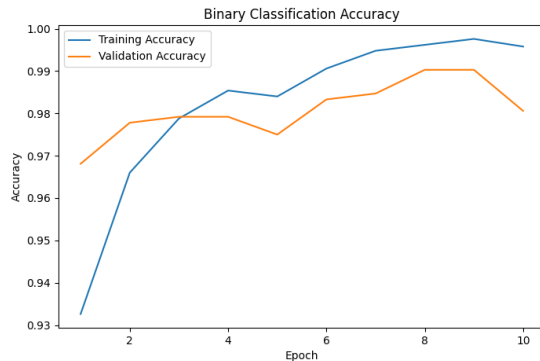


Fig. 11. The curve of the binary classification accuracy

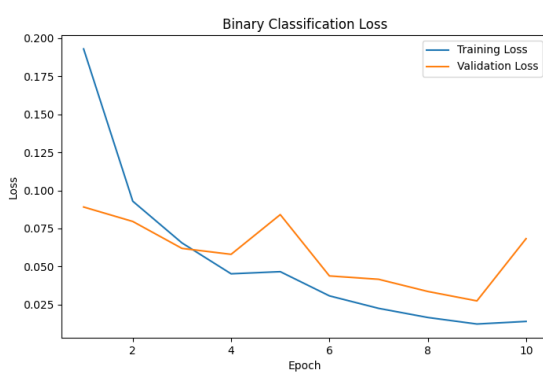


Fig. 12. The curve of the binary classification loss on preprocessed

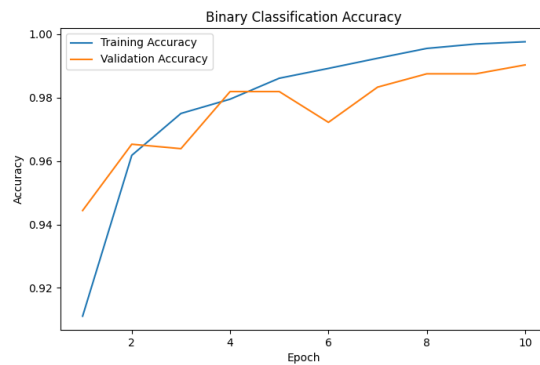


Fig. 13. The curve of the binary classification accuracy on preprocessed data

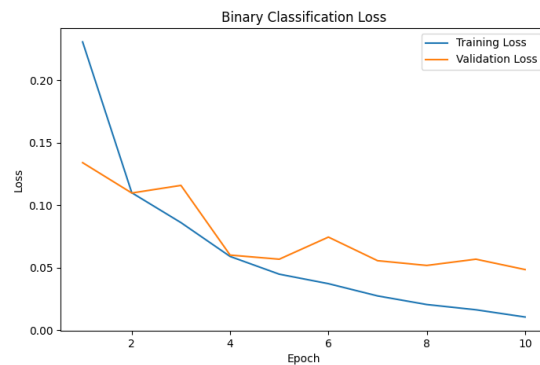


Fig. 14. The curve of the binary classification loss

214 **A.2. Applied on preprocessed data**

215 The model trained on the preprocessed dataset showed a clear
 216 improvement in both stability and overall performance. Starting
 217 from an initial accuracy of 91%, MobileNetV2 quickly progressed
 218 to 99% training accuracy and 99% validation accuracy by the
 219 final epoch. Loss values consistently decreased for both training
 220 and validation sets, and the high precision, recall, and F1-scores
 221 remained closely matched across epochs, indicating balanced
 222 predictions with minimal overfitting. Compared to the non-
 223 preprocessed experiment, the preprocessed version converged
 224 more cleanly, exhibited smoother accuracy and loss curves, and
 225 achieved slightly higher final validation performance. These
 226 results confirm that preprocessing enhanced feature consistency
 227 and helped the model generalize better while maintaining rapid
 228 convergence.

229 **B. Multi-Class Classification with MobileNetV2**

230 **B.1. Applied on data not preprocessed**

231 MobileNetV2 was trained to classify abnormal MRI scans into
 232 glioma, meningioma, or pituitary tumor categories. The model
 233 showed steady improvement over 10 epochs, reaching a training
 234 accuracy of 95.4% and a validation accuracy of 87.3%. F1-score,
 235 precision, and recall on the validation set were similarly high,
 236 indicating that the model reliably distinguishes between different
 237 tumor types. The training and validation loss decreased
 238 consistently, suggesting effective learning and good generalization,
 239 although the validation performance is slightly lower than
 240 training, which is expected in multi-class tasks due to higher
 241 complexity.

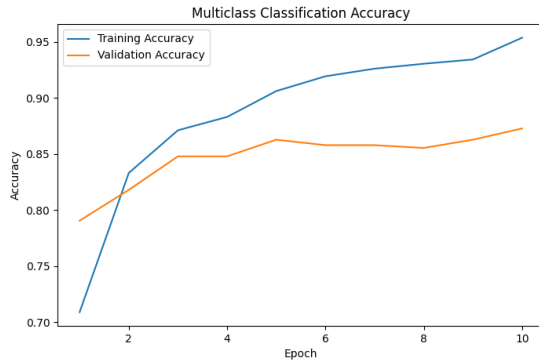


Fig. 15. The curve of the multi-class classification accuracy

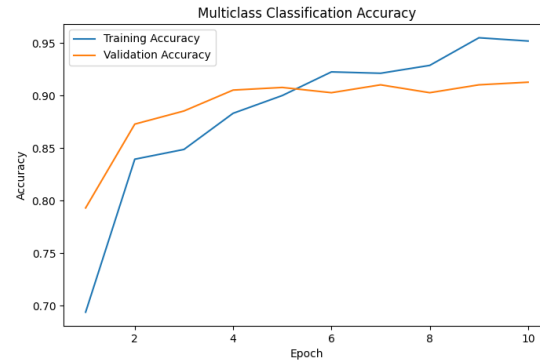


Fig. 17. The curve of the multi-class classification accurac after preprocessing

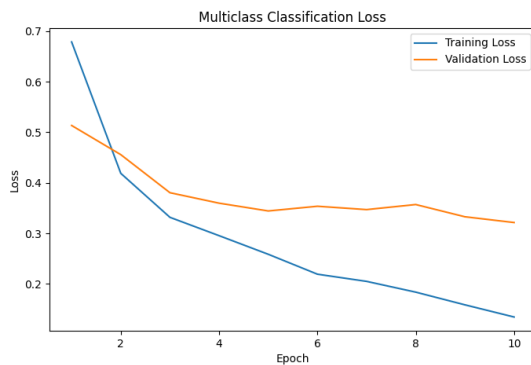


Fig. 16. The curve of the multi-class classification loss

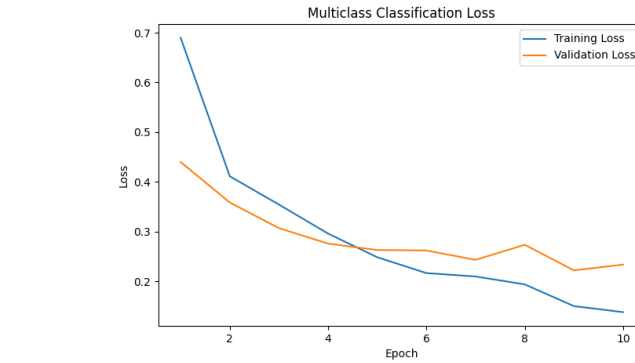


Fig. 18. The curve of the multi-class classification loss after preprocessing

C. Binary Classification with ResNet18

We trained ResNet18 as a binary classifier to distinguish between tumor and non-tumor MRI scans. The model converged quickly, achieving a test accuracy of 98%. Precision, recall, and F1-score metrics indicate strong discriminative ability, with precision for tumor and non-tumor at 1.00 and 0.93, recall at 0.97 and 1.00, and F1-score at 0.98 and 0.97, respectively. However, a noticeable gap between training and validation performance suggests some overfitting, likely due to the relatively small dataset size compared to ResNet18's large capacity. Dropout, early layer freezing, and balanced sampling mitigated overfitting to some extent, but the model's complexity exceeds the amount of available data, limiting generalization in edge cases.

D. Multi Classification with ResNet18

ResNet18 was trained to classify tumor MRI scans into glioma, meningioma, and pituitary tumor categories. The model reached 97% test accuracy, with pituitary tumors identified with near-perfect reliability. Most misclassifications occurred between glioma and meningioma due to their visual similarity. While precision, recall, and F1-score metrics were high across all classes, the large network exhibited signs of overfitting, with training accuracy consistently higher than validation accuracy. Fine-tuning only higher layers, combined with dropout and weight decay, helped control overfitting, but the relatively small dataset limited ResNet18's full generalization potential for multi-class tumor differentiation.

B.2. Applied on preprocessed data

Training the multiclass classifier on the preprocessed images led to a clear improvement in learning stability and overall performance. The model began with an accuracy of 69% but quickly progressed, reaching over 90% validation accuracy by the fourth epoch and stabilizing around 91% in the final iteration. Precision, recall, and F1-score followed the same trend, showing consistent and balanced predictions across all tumor categories. The loss steadily decreased for both training and validation sets, and the gap between them remained small, indicating controlled generalization without overfitting. Compared to the non-preprocessed setup, the preprocessed data enabled smoother convergence and higher final performance, confirming that the preprocessing pipeline strengthened feature quality and improved the model's ability to differentiate between the three tumor types.

283 E. Binary Classification with EfficientNetV2B0

284 Training and fine-tuning a large architecture like Efficient
 285 NetV2B0 on a relatively small dataset can easily lead to dramatic
 286 overfitting. The model's high capacity allows it to memorize
 287 training samples rather than generalize to unseen data, which
 288 can significantly reduce its reliability for brain tumor detection
 289 tasks when dataset size is limited.

290 F. Web Interface Demo

291 We conducted tests and demos using the MindScan interface
 292 with sample MRI images randomly from random internet
 293 sources for all tumor classes and no tumor class. The system
 294 successfully analyzed each case, providing accurate predictions
 295 and demonstrating reliable performance across different tumor
 296 types.

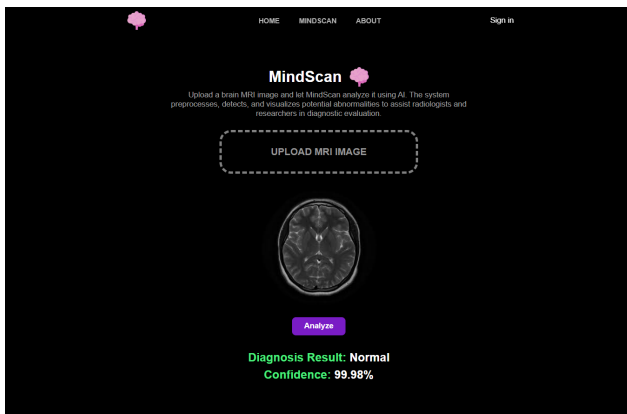


Fig. 19. Test in MindScan interface on a normal sample

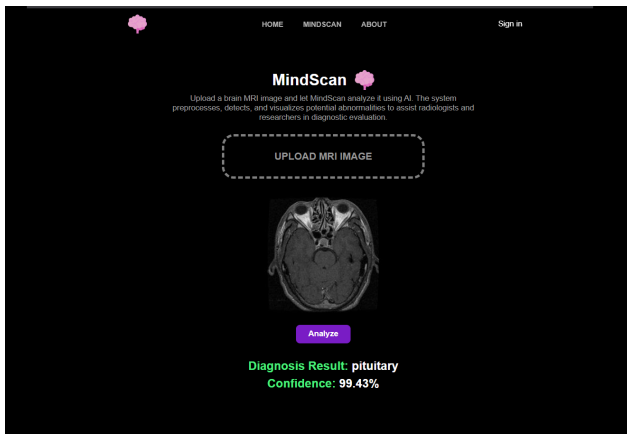


Fig. 20. Test in MindScan interface on an abnormal sample

297 4. DISCUSSION

298 A. MobileNetV2

299 A.1. Applied on data not preprocessed

300 The MobileNetV2-based pipeline performed well for both binary
 301 and multi-class brain tumor classification. Binary classification
 302 achieved near-perfect metrics, while multi-class classification
 303 reached 87.3% validation accuracy, showing reliable tumor type
 304 identification. The hierarchical design proved efficient, and Mo-
 305 bileNetV2's compact size supports fast, web-based deployment.

306 Slight gaps between training and validation suggest that more
 307 data or augmentation could further improve generalization.

308 A.2. Applied on preprocessed data

309 Applying preprocessing led to clear improvements in stability
 310 and overall performance for both binary and multiclass clas-
 311 sification. The binary model reached 99% validation accuracy
 312 with smooth convergence and minimal gaps between training
 313 and validation curves, indicating strong generalization. The
 314 multiclass model also benefited, achieving over 91% validation
 315 accuracy and maintaining consistent precision, recall, and F1-
 316 scores across all classes. Loss decreased steadily in both tasks,
 317 and the training process became more stable compared to the
 318 non-preprocessed setup. These results show that preprocessing
 319 enhanced feature clarity, improved convergence, and strength-
 320 ened MobileNetV2's ability to distinguish brain tumor types.

321 B. ResNet18

322 The ResNet18 pipeline showed strong performance in both bi-
 323 nary and multi-class classification but exhibited signs of overfit-
 324 ting due to the relatively small dataset compared to the model's
 325 large capacity. The binary classifier reached 98% accuracy with
 326 high precision and recall, effectively separating tumor and non-
 327 tumor images, though training accuracy was slightly higher
 328 than validation, indicating limited generalization in some cases.
 329 The multi-class classifier achieved 97% accuracy, with most er-
 330 rors occurring between glioma and meningioma. Freezing early
 331 layers and using regularization such as dropout and weight
 332 decay helped control overfitting, but the model's large architec-
 333 ture remains somewhat mismatched to the dataset size, making
 334 ResNet18 powerful but prone to overfitting when training on
 335 limited MRI data.

336 C. Comparison

337 MobileNetV2 trained on preprocessed data demonstrated the
 338 best overall performance for both binary and multi-class brain
 339 tumor classification. The model achieved 99% validation accu-
 340 racy for binary classification and 91.3% for multi-class clas-
 341 sification, with smooth convergence and minimal overfitting.
 342 Preprocessing clearly improved stability, generalization, and
 343 feature consistency, allowing the model to reliably distinguish
 344 tumor types. Its compact size and efficiency also make it ideal
 345 for real-time, web-based deployment, confirming MobileNetV2
 346 on preprocessed data as the optimal choice for this project.

Table 1. Training and Validation Metrics Across Epochs for MobileNetV2 and ResNet18^a

Model / Data	Train Acc	Val Acc	Train Loss	Val Loss
Binary Classification				
MNV2 (Raw)	0.9958	0.9806	0.0139	0.0683
MNV2 (PP)	0.9976	0.9903	0.0105	0.0485
Multi-Class Classification				
MNV2 (Raw)	0.9538	0.8728	0.1346	0.3215
MNV2 (PP)	0.9519	0.9127	0.1377	0.2334

^a Abbreviations: MNV2 = MobileNetV2, PP = Preprocessed, Acc = Accuracy, Val = Validation.

349 5. LIMITATIONS AND FUTURE WORK

350 Despite the strong performance of MindScan, several limitations exist. The dataset
351 used is relatively small and sourced from a single public repository, which may
352 limit the model's generalization to diverse clinical populations. Additionally, the
353 current system focuses solely on classification and does not provide tumor seg-
354 mentation, which could be valuable for treatment planning and surgical guidance.
355 Future work could address these limitations by incorporating larger, multi-center
356 datasets to improve generalization, adding automated tumor segmentation capa-
357 bilities, and exploring 3D MRI analysis. Further validation in real-world clinical
358 settings would also strengthen the system's reliability and applicability.

359 6. CONCLUSION

360 In this work, we developed MindScan, a web-based AI system for brain tumor
361 detection and classification using MRI images. The proposed hierarchical ap-
362 proach—binary classification to detect abnormalities followed by multi-class clas-
363 sification to identify tumor types—demonstrated strong performance, with Mo-
364 bileNetV2 achieving high accuracy, F1-score, precision, and recall. The system
365 provides real-time, reliable predictions while remaining lightweight and suitable
366 for web deployment. These results highlight the potential of AI-assisted tools to
367 support early and accurate diagnosis of brain tumors, improving clinical decision-
368 making and patient outcomes. Future work could focus on expanding the dataset,
369 adding segmentation capabilities, and validating the model across diverse clinical
370 settings.

371 REFERENCES

- 372 1. R. R. S. Selva Birunda, M. Kaliappan, Taylor Francis Online (2025).
<https://doi.org/10.1080/01616412.2025.2574357>.
- 373 2. C. R. B. M. C. Nuthi Raju, Kankanala Srinivas, ScienceDirect (2025).
<https://doi.org/10.1016/j.aej.2025.10.019>.
- 374 3. J. A. . M. A. S. Abdu Alhaji Jamaa, Anum Kamal, Springer Nat. Link
375 (2025). <https://link.springer.com/article/10.1007/s40435-025-01887-0>.
- 376 4. K. M. I. Group, "Brain mri images for brain tumor detection
377 dataset," (2022). <https://www.kaggle.com/datasets/masoudnickparvar/brain-tumor-mri-dataset?resource=download&select=Training>.
- 378 5. DarttGoblin, "Mindscan server repository," https://github.com/DarttGoblin/MindScan_server (2025). Accessed: 2025-12-05.
- 379 6. M. Sandler, A. Howard, M. Zhu, *et al.*, "Mobilenetv2: Inverted residuals
380 and linear bottlenecks," in *Proceedings of the IEEE/CVF Conference on
381 Computer Vision and Pattern Recognition (CVPR)*, (2018), pp. 4510–
382 4520.
- 383 7. K. He, X. Zhang, S. Ren, and J. Sun, "Deep residual learning for image
384 recognition," in *Proceedings of the IEEE Conference on Computer
385 Vision and Pattern Recognition (CVPR)*, (2016), pp. 770–778.
- 386 8. M. Tan and Q. V. Le, "Efficientnetv2: Smaller models and faster training,"
387 in *Proceedings of the International Conference on Machine Learning
388 (ICML)*, (2021), pp. 10096–10106.
- 389 9. DarttGoblin, "Mindscan web interface," <https://darttgoblin.github.io/MindScan/MindScan.html> (2025). Accessed: 2025-12-05.